

# Orbital magnetic moments and magnetic anisotropy energy in $\text{Rh}_N$ and $\text{Co}_N\text{Pd}_M$ clusters

R. Guirado-López<sup>1</sup>, P. Villaseñor-González<sup>1</sup>, J. Dorantes-Dávila<sup>1,2</sup>, and G.M. Pastor<sup>2,a</sup>

<sup>1</sup> Instituto de Física, Universidad Autónoma de San Luis Potosí, San Luis Potosí, Mexico

<sup>2</sup> Laboratoire de Physique Quantique<sup>b</sup>, Université Paul Sabatier, 31062 Toulouse Cedex, France

Received 10 September 2002

Published online 3 July 2003 – © EDP Sciences, Società Italiana di Fisica, Springer-Verlag 2003

**Abstract.** The orbital magnetic moments  $\langle L \rangle$  and the magnetic anisotropy energy (MAE) of  $\text{Rh}_N$  ( $N \leq 55$ ) and  $\text{Co}_{19}\text{Pd}_M$  ( $M = 24$  and  $60$ ) are determined by using a self-consistent real-space tight-binding method. For  $\text{Rh}_N$ ,  $\langle L \rangle$  amounts typically 20–50% of the total magnetic moment  $M_z = 2\langle S_z \rangle + \langle L_z \rangle$ . Strong oscillations as a function of  $N$  are observed with a rapid convergence to zero as the spin magnetization vanishes for  $N \simeq 40$ –50. In  $\text{Co}_{19}\text{Pd}_M$  clusters, the magnetization per Co atom is remarkably larger than in pure  $\text{Co}_{19}$ . This is mainly due to the local spin moments  $\langle S_{iz} \rangle$  induced at the Pd atoms, which amount to about 20% of the spin moment per Co atom [ $2\langle S_{iz} \rangle_{\text{Pd}} = (0.1\text{--}0.3)\mu_B$ ]. Large orbital moments are found at the Co atoms, particularly at the Co/Pd interface. The anisotropy of  $\langle L \rangle$  and the associated MAE's are analyzed from a local perspective.

**PACS.** 36.40.Cg Electronic and magnetic properties of clusters – 75.10.Lp Band and itinerant models

## 1 Introduction

Two of the main characteristics of a magnetic material are the ground-state magnetic moments, which define the saturation magnetization, and the magnetic anisotropy energy which determines the low-temperature orientation of the magnetization  $\mathbf{M}$  and its stability. On the one side, the sources of magnetism are the currents associated to the electronic motion, or orbital moments, and the electron's intrinsic spin. On the other side, the dependence of the electronic structure and magnetic properties on the orientation of  $\mathbf{M}$  is dominated by the spin-orbit interactions. In particular, the MAE – defined as the energy difference involved in turning  $\mathbf{M}$  from the low-energy direction, or easy axis, to a high-energy direction, or hard axis – is a magnitude of crucial importance in view of technological applications like magnetic recording or memory devices. The control and understanding of these properties at a microscopic level are central to the development of magnetic nanostructures.

Investigations of orbital magnetism in low-dimensional systems – in the way from the atom to the solid – show that the orbital moments are very sensitive to the local environment of the atoms [1–8]. For example, calculations on transition metals (TM) surfaces, have revealed an important enhancement of the local orbital moments  $\langle L(i) \rangle$ , which is in general larger at open surfaces than at the more compact ones [7]. In the case of free clusters, very little is known about orbital magnetism, particularly from

the point of view of theory, which has been so far concerned mainly with the dominant spin contributions. Recent self-consistent calculations show that the reduction of system size causes a remarkable enhancement of  $\langle L \rangle$  with respect to the bulk [8]. For example, in  $\text{Ni}_N$  with  $N \leq 13$  one obtains values about eight times larger than  $\langle L \rangle(\text{bulk}) = 0.05\mu_B$ . On the other side, comparison with the atomic result  $L(\text{atom}) = 2\mu_B$  shows that the largest part of the quenching of  $L$  takes place already at the smallest sizes, as soon as full rotational symmetry is lost.

These results anticipate interesting size and structural dependence of the orbital moments in other systems particularly in the case of  $4d$  transition metal elements, which are non-magnetic in bulk and show weak, non-saturated magnetism [9–12]. The  $4d$  elements are characterized by significant spin-orbit couplings (larger than the  $3d$  ones) which give rise to a new class of magnetic materials with particularly enhanced magneto-crystalline anisotropies. In addition, bimetallic clusters formed with  $3d$  and  $4d$  elements like Co–Pd systems are particularly appealing due to the strong magnetic susceptibility of Pd and the remarkably rich magneto-anisotropic behavior of the Co/Pd interfaces [13, 14]. It is the purpose of this communication to investigate the MAE and orbital magnetic moments of  $\text{Rh}_N$  and  $\text{Co}_N\text{Pd}_M$  clusters as a function of  $N$  and  $M$  by considering representative cluster structures.

## 2 Model

The calculations are based on the self-consistent tight-binding method developed in references [7, 15].

<sup>a</sup> e-mail: [gustavo.pastor@irsamc.ups-tlse.fr](mailto:gustavo.pastor@irsamc.ups-tlse.fr)

<sup>b</sup> UMR 5626 du CNRS

The electronic Hamiltonian is given by the sum of three terms

$$H = H_0 + H_C + H_{SO}. \quad (1)$$

$H_0$  refers to the inter-atomic hopping term that describes the single-particle spectrum. The Coulomb interaction  $H_C$  is treated in the unrestricted Hartree-Fock approximation:

$$H_C = \sum_{im\sigma} \Delta\varepsilon_{im\sigma} \hat{n}_{im\sigma}, \quad (2)$$

where  $\hat{n}_{im\sigma} = \hat{c}_{im\sigma}^\dagger \hat{c}_{im\sigma}$  is the electron-number operator and

$$\Delta\varepsilon_{im\sigma} = \sum_{m'} (U_{mm'} - \frac{J_{mm'}}{2}) \nu_{im'} - \frac{\sigma}{2} \sum_{m'} J_{mm'} \mu_{im'} \quad (3)$$

are the orbital- and spin-dependent shifts of the  $d$  levels at atom  $i$ . Notice that the direct and exchange Coulomb integrals  $U_{mm'}$  and  $J_{mm'}$  depend on  $m$  due to the angular dependence of the atomic-like orbitals. In this way atomic symmetry is strictly respected and all atomic Hund's rules are naturally derived (see, for example, Ref. [16]). The third term in equation (1) refers to the spin-orbit interaction [15,17]

$$H_{SO} = - \sum_{i,\alpha\sigma,\beta\sigma'} \xi_i (\mathbf{L}_i \cdot \mathbf{S}_i)_{\alpha\sigma,\beta\sigma'} \hat{c}_{i\alpha\sigma}^\dagger \hat{c}_{i\beta\sigma'}, \quad (4)$$

where  $(\mathbf{L}_i \cdot \mathbf{S}_i)_{\alpha\sigma,\beta\sigma'}$  are the intra-atomic matrix elements of  $\mathbf{L} \cdot \mathbf{S}$  that couple the up and down spin-manifolds and which depend on the orientation of the magnetization with respect to the cluster structure.

The local densities of electronic states (DOS)  $\rho_{im\sigma}^\delta(\varepsilon)$  are determined self-consistently for each orientation  $\delta$  of the spin magnetization  $\mathbf{S}$ . In this paper we consider  $\delta = z$ , usually along a principal  $C_n$  symmetry axis of the cluster, and  $\delta = x$  along a nearest neighbor (NN) bond perpendicular to  $z$ . The associated single-particle problem is solved by using the Haydock-Heine-Kelly's recursion method [18].

Once selfconsistency is achieved, the average local orbital moments  $\langle L_{i\delta} \rangle$  at atom  $i$  are calculated from

$$\langle L_{i\delta} \rangle = \sum_{\sigma} \sum_{m=-2}^2 \int_{-\infty}^{\varepsilon_F} m \rho_{im\sigma}^\delta(\varepsilon) d\varepsilon, \quad (5)$$

where  $m$  indicates the magnetic quantum number. The quantization axis of the orbital momentum is thereby taken to be the same as the spin quantization axis.

The electronic energy per atom

$$E_\delta = \frac{1}{N} \sum_i E_\delta(i) \quad (6)$$

can be written as the sum of local contributions

$$E_\delta(i) = \sum_{m\sigma} \left[ \int_{-\infty}^{\varepsilon_F} \varepsilon \rho_{im\sigma}^\delta(\varepsilon) d\varepsilon - E_{im\sigma}^{\text{dc}} \right] \quad (7)$$

corresponding to each atom  $i$  of the cluster. Here,  $E_{im\sigma}^{\text{dc}} = (1/2)\Delta\varepsilon_{im\sigma} \langle \hat{n}_{im\sigma} \rangle$  stands for the double-counting correction. The MAE is defined as  $\Delta E_{xz} = E_x - E_z$ , *i.e.*, as the change in the electronic energy  $E_\delta$  associated to a change in the orientation of the magnetization. Taking advantage of the local formulation one may express

$$\Delta E_{xz} = \sum_i \Delta E_{xz}(i) \quad (8)$$

as a sum of atom-resolved contributions

$$\Delta E_{xy}(i) = E_x(i) - E_z(i), \quad (9)$$

where  $E_\delta(i)$  is given by equation (7). In this way the magneto-anisotropic properties can be related to the various local atomic environments.

### 3 Results and discussion

The parameters used for the calculations are determined as follows. The two center  $d$ -electron hopping integrals are given by the canonical expression in terms of the corresponding bulk  $d$ -band widths [ $W_b(\text{Co}) = 5.5$  eV,  $W_b(\text{Pd}) = 5.9$  eV, and  $W_b(\text{Rh}) = 7.4$  eV]. The intra-atomic direct and exchange Coulomb integrals  $U_{mm'}$  and  $J_{mm'}$  are given in terms of the atomic two-electron integrals  $F^{(0)}$ ,  $F^{(2)}$ , and  $F^{(4)}$  [16]. The ratios  $F^{(0)}/F^{(2)}$  and  $F^{(4)}/F^{(2)}$  are taken from atomic Hartree-Fock calculations [19]. For Co the average exchange integral  $J_{\text{av}} = (49F^{(2)} + 441F^{(4)})/14$  is chosen to yield the proper  $T = 0$  magnetic moment in the bulk. In the case of Rh and Pd, we use  $J_{\text{av}}^{\text{Rh}} = 0.48$  eV and  $J_{\text{av}}^{\text{Pd}} = 0.52$  eV, which have been obtained from density functional calculations (Stoner theory) taking into account correlation effects beyond the local spin density approximation [20]. The SO-coupling constants  $\xi(\text{Co}) = 0.088$  eV,  $\xi(\text{Pd}) = 0.190$  eV, and  $\xi(\text{Rh}) = 0.180$  eV are taken from reference [17]. Concerning the cluster geometries, we consider representative fcc clusters formed by a central atom and its successive shells of NN's. In the case of  $\text{Co}_N\text{Pd}_M$  this corresponds to a Co core covered by several Pd shells. Examples of these structures are illustrated in reference [11].

For  $\text{Rh}_N$  clusters, the calculated spin magnetic moments agree within 5–10% with previous calculations in which SO-interactions were neglected [11]. The small differences found are probably due to the SO-induced additional broadening of the local densities of states that often lead to slightly smaller spin moments. For the largest sizes ( $N > 19$ ) an antiferromagnetic-like state is obtained in most of the particles. This is consistent with the experimentally observed decrease to a zero net magnetization as  $N$  increases.

In Figure 1 results are given for the size dependence of the average orbital magnetic moment per atom

$$\langle L_\delta \rangle = \frac{1}{N} \sum_i L_\delta(i) \quad (10)$$

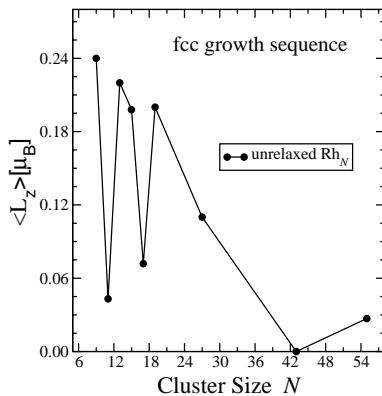


**Fig. 1.** Average orbital moment in fcc  $\text{Rh}_N$  clusters as a function of the cluster size  $N$  as obtained assuming bulk NN distances. The calculated points are indicated by the dots and the lines are a guide to the eye. Additional oscillations for intermediate  $N$  cannot be excluded.

of  $\text{Rh}_N$  clusters having fcc-like structures and bulk NN distances. These correspond to the  $\delta = z$  magnetization direction along a  $C_4$  axis of the fcc structure. In the present case only small differences are obtained for other magnetization directions due to the high symmetry of assumed cluster geometry. The calculations show significant orbital moments  $\langle L_\delta \rangle = (0.1\text{--}0.24)\mu_B$  for  $N \leq 19$  which are similar to what is found in  $\text{Ni}_N$  [8,21]. Quantitatively, the contribution of  $\langle L_\delta \rangle$  to the total magnetic moment amounts to about 20–50% [23]. In addition  $\langle L_\delta \rangle$  displays strong oscillations as a function of cluster size  $N$  which are mainly a consequence of the rapid decrease of the spin magnetization with increasing  $N$  and of the presence of weak (unsaturated) itinerant magnetism [22]. Indeed, these two effects yield strong changes in the energy-level distribution around the Fermi energy and thus a remarkable size dependence of  $\langle L \rangle$  is obtained.

As examples of bi-metallic clusters we consider  $\text{Co}_{19}\text{Pd}_M$  with  $M \leq 60$  assuming for simplicity Co bulk NN's bond lengths. The total magnetic moments per Co atom  $M_\delta$  are remarkably large for all the considered sizes (*e.g.*,  $M_z = 2.22\mu_B$  and  $2.1\mu_B$  for  $M = 24$  and 60, respectively). The magnetization  $M_\delta$  of  $\text{Co}_N\text{Pd}_M$  can be regarded as the result of three major effects. The first and leading contribution is given by the spin moments of the Co atoms  $i = 1\text{--}N$ . For Co atoms in the inner shells one obtains saturated spin moments  $2\langle S_z \rangle \simeq 1.6\mu_B \simeq 10 - n_d$ , while the Co atoms at the Co–Pd interface present somewhat smaller unsaturated spin moments  $2\langle S_z \rangle \simeq 1.5\mu_B$ . The second important contribution to  $M_\delta$  are the local spin moments induced at the Pd atoms of the Co–Pd interface (*e.g.*, for  $M = 24$ ,  $2\langle S \rangle_{\text{Pd}} = 0.30\text{--}0.35\mu_B$ ). As the thickness of the  $\text{Pd}_M$  shell increases the local coordination number of the Pd atoms increases and a partial reduction of  $\langle S \rangle_{\text{Pd}}$  is observed (*e.g.*, for  $M = 60$ ,  $2\langle S \rangle_{\text{Pd}} \simeq 0.13\mu_B$ ). Finally, the third main part of the calculated magnetization is given by the orbital magnetic moments  $\langle L_\delta \rangle$ , which are always parallel to the spin moments, as corresponds to elements having a  $d$ -shell that is more than half filled. The calculated average orbital moments per Co

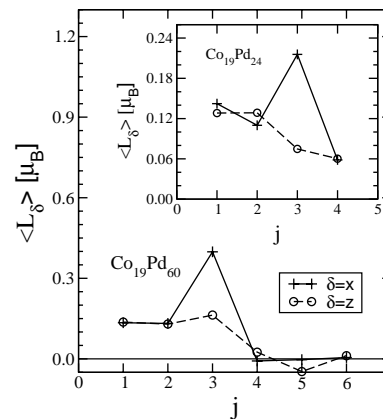


**Fig. 2.** Local orbital magnetic moments along the spin magnetization direction in fcc-like  $\text{Co}_{19}\text{Pd}_M$  clusters with  $M = 24$  and 60. The results refer to the average at each NN shell  $j$  surrounding the central atom  $j = 1$ .  $\delta = x$  and  $z$  indicate different spin magnetization directions as described in the text. The shells  $j \leq 3$  ( $j \geq 4$ ) correspond to Co (Pd) atoms.

atom are  $\langle L \rangle = 0.23\mu_B$  for  $\text{Co}_{19}\text{Pd}_{24}$  and  $\langle L \rangle = 0.31\mu_B$  for  $\text{Co}_{19}\text{Pd}_{60}$ . Note that these values are enhanced by more than 100% with respect to the Co-bulk orbital moment.

The environment dependence of the local orbital moments  $\langle L_\delta \rangle(j)$  provides further insight on the magnetic behavior of bimetallic clusters. Figure 2 displays  $\langle L_\delta \rangle(j)$  in the considered Co–Pd clusters, where  $j = 1$  refers to the central atom and  $j > 1$  to the successive NN shells of the fcc structure. The sites  $j \leq 3$  ( $j \geq 4$ ) correspond to Co (Pd) atoms. One observes that  $\langle L_\delta \rangle(j)$  generally increases with  $j$ , showing some oscillations as we move from the center to the surface of the cluster. Notice the particularly large value of  $\langle L_x \rangle(3)$  of the the Co atoms at the interface:  $\langle L_x \rangle(j = 3) \simeq 0.39\mu_B$  for  $\text{Co}_{19}\text{Pd}_{60}$  (main figure) and  $\langle L_x \rangle(j = 3) \simeq 0.22\mu_B$  for  $\text{Co}_{19}\text{Pd}_{24}$  (inset). Thus, a thicker Pd shell results in a larger  $\langle L_\delta \rangle$  at the interface. This trend is opposite to the one observed in the spin moments and demonstrates the importance of the Co–Pd interface to orbital magnetism.

The anisotropy of  $\langle L_\delta \rangle(j)$  reflects the anisotropy of SO interactions from a local point of view. Our results show significant  $\Delta L = \langle L_x \rangle(j) - \langle L_z \rangle(j)$  with the largest values being found at the interface Co atoms. This is consistent with the large MAE's per Co atom  $\Delta E_{xy} = E_x - E_z$  shown in Table 1. Indeed, the local contribution of the outermost Co shell to the MAE stabilizes the  $x$ -direction of the magnetization ( $\Delta E_{xy} < 0$  for  $j = 3$  in Tab. 1). This holds for all considered values of  $M \geq 24$ . Therefore, the Co–Pd interface plays a main role in determining the stable magnetization direction of the system. A similar behavior has been observed in Co–Pd films [13,14]. Qualitatively, the environment dependence of  $\Delta E_{xy}$  can be regarded as the result of two main effects: the changes in the electronic structure of the Co cluster due to Co–Pd hybridizations, and the contribution of the interface Pd atoms which carry small magnetic moments.

In conclusion, the magnetic anisotropy energy and orbital magnetic moments of  $\text{Rh}_N$  and  $\text{Co}_N\text{Pd}_M$

**Table 1.** Local magnetic anisotropy energy  $\Delta E_{xy}(j) = E_x(j) - E_z(j)$  (in meV's) in fcc-like  $\text{Co}_{19}\text{Pd}_M$  clusters with Co-bulk NN bond-lengths. The results correspond to the average at each NN shell  $j$  surrounding the central atom  $j = 1$ .  $\Delta E_{xy}$  stands for the total magnetic anisotropy energy per Co atom [see Eqs. (7–9)].

$M$	$j = 1$	$j = 2$	$j = 3$	$j = 4$	$j = 5$	$j = 6$	$\Delta E_{xy}$
0	-1.6	0.5	0.3				0.36
24	3.0	-1.9	-7.1	1.9			-0.81
36	0.6	-1.9	-6.1	5.3	-6.1		-0.32
60	1.0	-1.7	-4.1	3.7	-3.9	-0.3	-0.38

clusters have been investigated in the framework of a self-consistent tight-binding model Hamiltonian including spin-orbit interactions. The hybridizations between a magnetic transition metal like Co and a highly polarizable element like Pd have been shown to be crucial for the magneto-anisotropic behavior of heterogeneous clusters. In future, it would be also of interest to consider other geometrical configurations of bi-metallic clusters, such as a Pd core capped with Co shells, and to contrast the resulting behaviors. Comparison with experiment could then be used to infer information on the morphology of alloy clusters from their magnetic properties. Research in this direction is currently in progress.

This work was financed in part by the EU GROWTH project AMMARE under contract number G5RD-CT-2001-00478 and by CONACyT (Mexico) through grants 32085E and W-8001-millennium. J.D.D. acknowledges support from the grant FIES-98-101-I of IMP (Mexico).

## References

1. J. Trygg *et al.*, Phys. Rev. Lett. **75**, 2871 (1995); M. Tischer *et al.*, *ibid.*, 1602 (1995); D. Weller *et al.*, *ibid.*, 3752 (1995); A.N. Anisimov *et al.*, *ibid.* **82**, 2390 (1999)
2. P. Ohresser, N.B. Brookes, S. Padovani, F. Scheurer, H. Bulou, Phys. Rev. B **64**, 104429 (2001)
3. P. Gambardella *et al.*, Nature **416**, 301 (2002)
4. C. Binns, Surf. Sci. Rep. **44**, 1 (2001)
5. T. Koide *et al.*, Phys. Rev. Lett. **87**, 257201 (2001)
6. J.T. Lau *et al.*, Phys. Rev. Lett. **89**, 057201 (2002)
7. J.L. Rodriguez-López, J. Dorantes-Dávila, G.M. Pastor, Phys. Rev. B **57**, 1040 (1998)
8. R.A. Guirado-López, J. Dorantes-Dávila, G.M. Pastor, to be published
9. A.J. Cox, J.G. Louderback, L.A. Bloomfield, Phys. Rev. Lett. **71**, 923 (1993); A.J. Cox, J.G. Louderback, S.E. Apsel, L.A. Bloomfield, Phys. Rev. B **49**, 12295 (1994)
10. B.V. Reddy, S.N. Khanna, B.I. Dunlap, Phys. Rev. Lett. **70**, 3323 (1993)
11. P. Villaseñor González, J. Dorantes-Dávila, G.M. Pastor, H. Dreyssé, Phys. Rev. B **55**, 15084 (1997)
12. D. Zitoun *et al.*, Phys. Rev. Lett. **89**, 037203 (2002)
13. J. Kohlhepp, U. Gradmann, J. Magn. Magn. Mater. **139**, 347 (1995)
14. J. Dorantes-Dávila, H. Dreyssé, G.M. Pastor, to be published
15. G.M. Pastor, J. Dorantes-Dávila, S. Pick, H. Dreyssé, Phys. Rev. Lett. **75**, 326 (1995)
16. J.C. Slater, *Quantum Theory of Atomic Structure* (McGraw-Hill Book Co., Inc., N. Y., 1960), Vols. I and II
17. P. Bruno, *Magnetismus von Festkörpern und Grenzflächen*, Ferienkurse des Forschungszentrums Jülich (KFA Jülich, 1993), ISBN 3-89336-110-3, Chap. 24
18. R. Haydock, in *Solid State Physics*, edited by H. Ehrenreich, F. Seitz, D. Turnbull (Academic, New York, 1980), Vol. 35, p. 215
19. J.B. Mann, *Atomic Structure Calculations* (Los Alamos Sci. Lab., Rept. LA-3690, 1967)
20. N.E. Christensen, O. Gunnarsson, O. Jepsen, O.K. Andersen, J. Phys. (Paris) **49**, C8-17 (1988); O.K. Andersen, O. Jepsen, D. Glötzel, *Highlights of Condensed Matter Theory*, edited by F. Bassani, F. Fumi, M.P. Tosi (North Holland, Amsterdam, 1985), p. 59
21. Preliminary results for different structures show that the enhancement of  $\langle L_\delta \rangle$  is even more pronounced in open and low symmetry geometries, for example, in bcc- or icosahedral-like structures
22. The magnetic anisotropy energy of  $\text{Rh}_N$  also shows a strong size dependence with oscillations in magnitude as well as changes of sign. This should have direct consequences on the magnetic properties at low temperatures, since it implies that the easy and hard axis change as the size of the cluster increases
23. Calculations allowing structural relaxation in  $\text{Rh}_N$  yield significant bond-length contractions which reduce part of the enhancement of  $\langle L_\delta \rangle$ . Still, the orbital contributions in the relaxed geometries remain about 15–25% of the total magnetic moment